Evaluation of Surface Composition of Surface Active Water−Alcohol Type Mixtures: A Comparison of Semiempirical Models

Martta Salonen,[†] Jussi Malila,[‡] Ismo Napari,*[,†] and Ari Laaksonen[‡]

Department of Physical Sciences, University of Helsinki, P.O. Box 64, FIN-00014 Helsinki, Finland, and Department of Applied Physics, University of Kuopio, P.O. Box 1627, FIN-70211 Kuopio, Finland

Received: June 3, 2004; In Final Form: November 8, 2004

We study adsorption at planar liquid−vapor interface of surface active binary mixtures and test three well-known models for the composition of surface phase. The models were originally presented by Guggenheim [*Thermodynamics*, 3rd ed.; North Holland: Amsterdam, 1967], Eberhart [*J. Phys. Chem.* **1966**, *70*, 1183], and Laaksonen and Kulmala [*J. Chem. Phys.* **1991**, *95*, 6745]. These are compared to results for model fluids from density functional theory (DFT). The model of Laaksonen and Kulmala is in best agreement with DFT calculations. Surface mole fraction of the solute component from the Guggenheim model exceeds one for a mixture with high surface activity. The failure of the Guggenheim model is also evident in our calculations for water−methanol, water−ethanol, and water−*n*-propanol mixtures.

1. Introduction

Water−surfactant mixtures are used for a variety of purposes in modern society, for example as cleaning agents and solvents, but they also are important to biological systems, e.g., to gas exchange in pulmonary tissues (e.g., ref 1). In atmospheric sciences they are of great importance in phenomena ranging from cloud droplet activation and aerosol health effects all the way down to theories describing the emergence of life.[2−4]

In atmospheric applications surface active substances are often found in processes involving nucleation, e.g., formation of small liquidlike droplets in a supersaturated vapor phase. A practical approach to study nucleation is classical nucleation theory, which, however, has well-known deficiencies. Most revealing comparisons between theory and experiment in water−surfactant nucleation have been done using water−alcohol mixtures.[5,6] Water−alcohol mixtures are a convenient choice for this purpose because their thermodynamical properties are well-known (see section 3). These studies, as well as work done on model mixtures,[7,8] have shown that classical binary nucleation theory of water−surfactant (alcohol) mixtures show unphysical behavior that is connected to the description of surface composition of the mixtures.[9] On the other hand, a phenomenological model that describes the surface composition explicitly[7,10] does not suffer from such problems. It is therefore of interest to study the predictions of such phenomenological models of the surface composition in detail and to compare them to molecular theories and experimental data. In this paper we concentrate on testing and comparing models in the case of planar liquid−vapor interfaces.

Several phenomenological models exist for prediction of surface compositions of binary fluids (e.g., refs 7, 11, and 12). Recently, Raina and co-workers[13,14] studied the surface compositions of water−alcohol mixtures experimentally and found that a simple phenomenological model suggested by us some years ago predicted their results quite well. The concept of surface composition is in some sense not very well-defined, as it can refer to local compositions along the smoothly varying density profiles at the surface, to compositions averaged over some finite slices over the density profiles, or to compositions expressed using surface excesses in the Gibbsian sense. Usually, experimental methods measure compositions averaged over varying distances (depending on the method), and the excess quantities appearing in the Gibbs adsorption equation are not obtained directly. Here, we study the local, averaged, and excess quantities of model surface active fluids using density functional theory and compare the predictions of different phenomenological models with the DFT calculations. We also compare the phenomenological model predictions for water−alcohol systems.

2. Models for Surface Composition

The Guggenheim model for surface adsorption is based on the Gibbs adsorption equation and information on the area occupied by each molecular species on the surface.[15,11] At constant temperature one obtains from the adsorption equation

$$-\frac{\partial\gamma}{\partial x_b} = \Gamma_1 \frac{\partial\mu_1}{\partial x_b} + \Gamma_2 \frac{\partial\mu_2}{\partial x_b} \tag{1}$$

where Γ_i is the surface number of molecules per unit area, x_b is the bulk mole fraction of component 2, $\mu_{i,s}$ is chemical potential at the surface, and γ is the surface tension of a planar gas−liquid interface. For surfaces that are in thermodynamical equilibrium

$$\mu_{i,s} = \mu_{i,b} \equiv \mu_i, \quad \forall i \tag{2}$$

and the notation above is consistent with general terminology in thermodynamics.

Equation 1 alone is not sufficient to determine both Γ_1 and Γ_2. Guggenheim proceeded to assume that the interfacial layer is unimolecular and each molecule of the same species takes up a constant area on the interface. Then

$$A_1\Gamma_1 + A_2\Gamma_2 = 1 \tag{3}$$

where A_i is the partial molecular area of the component i on the surface.

[†] University of Helsinki.
[‡] University of Kuopio.
* Corresponding author.

10.1021/jp047610w CCC: $30.25
Published on Web 02/01/2005

Guggenheim considered water−ethanol mixtures, assigned values for A_i by assuming that the long axis of the ethanol molecule is positioned perpendicular to the surface,[15] and obtained a series of calculated data points for the surface mole fraction $x_s = \Gamma_2/(\Gamma_1 + \Gamma_2)$ which seemed to validate this simple and appealing model. A similar model has later been used also by other authors.[16−18]

Eberhart[12] assumed that the surface tension of a mixture can be expressed as a linear combination of the surface tensions of the pure components γ_1 and γ_2:

$$\gamma(x_b) = (1 - x_s)\gamma_1 + x_s\gamma_2 \tag{4}$$

Knowing $\gamma(x_b)$, one can calculate x_s from eq 4. Laaksonen and Kulmala[7] modified this approach by weighing the surface mole fractions with the partial molecular volumes of pure components v_1 and v_2:

$$\gamma(x_b) = \frac{(1 - x_s)v_1\gamma_1 + x_s v_2\gamma_2}{(1 - x_s)v_1 + x_s v_2} \tag{5}$$

Equations 4 and 5 can in fact be derived if the liquid is considered a regular lattice with the surface phase represented by a monolayer where molecules of type 1 occupy one lattice site and molecules of type occupy r connected lattice sites.[19] By equating the chemical potentials of bulk and surface phases and assuming that the solution is athermal, one can derive[19]

$$\gamma(x_b) = \gamma_1\phi_1^l + \gamma_2\phi_2^l \tag{6}$$

where ϕ_1^l and ϕ_2^l are the volume fractions in the bulk liquid. However, eq 6 is only valid if the volume fractions in the bulk are equal to those in the surface layer. One can thus write the same equation in terms of the corresponding surface quantities. Equation 6 then leads to eq 5 and, if the molecules are of the same size, finally reduces to Eberhart's formula.

In addition to the three models presented here, there are also other models to estimate surface composition. For a partial review see ref 13.

3. Thermodynamic Variables for Water−Alcohol Mixtures

Surface tensions for water−alcohol mixtures were determined by fitting ln γ to a fractional−polynomial model using data given by Teitelbaum et al.[20] and reviewed by Timmermans.[21] The fits showed good accuracy in comparison with more recent data.[18,22,23]

For water−methanol and water−ethanol mixtures a density fit of the mixture was determined by a method presented by Vesala[24] using pure compound data.[21,25] For the water−*n*-propanol mixture, a density fit based on published data[21,25,26] was used, and it showed good accuracy in comparison with other available experimental data.[27]

The liquid-phase activity coefficients for water−methanol mixture were determined using van Laar coefficients taken from refs 28 and 29. For the water−ethanol mixture, three different approaches were used to determine activity coefficients: (i) van Laar coefficients[23] fitted on the data used by Guggenheim,[11] (ii) three-parameter Redlich−Kister equation of d'Avila and Silva,[30] and (iii) formulation presented by Gaulhofer et al.[31] which, despite of its apparent accuracy, does not obey the Gibbs−Duhem equation $(1 - x_b)\partial \ln f_1/\partial x_b + x_b\partial \ln f_2/\partial x_b = 0$, where f_1 and f_2 are the activity coefficients. In the case of the water−*n*-propanol mixture, two different sets of van Laar coefficients for liquid-phase activity coefficients were taken from ref 23 and from refs 28 and 29.

TABLE 1: Partial Molecular Areas for Water and Short-Chain *n*-Alcohol Molecules A_i (nm^2) at 298 K

A_1	A_2	reference
0.070	0.200	11
0.061	0.073	17
	>0.200	23[a]
0.066	0.133	16
	>0.240	33[a]

[a] Here value for A_2 was determined via eq 11.

For water−alcohol mixtures, chemical potentials are calculated via activity coefficients as $\mu_i = kT \ln a_i(x_b,T)$, where activity is defined as $a_i = f_{i,b}x_{i,b}$. For surface phase activities one has to note that bulk and surface phase activities are equal if and only if the surface phase chemical potential is defined via equations

$$\mu_{i,s} = \left(\frac{\partial G_s}{\partial n_{i,s}}\right)_{T,p,\gamma,n_{j,s}} \quad \text{and} \quad \mu_{i,s} = kT \ln f_{i,b}x_{i,b} \tag{7}$$

So the formula for surface phase activities used e.g. in refs 16 and 17

$$a_{i,s} = a_{i,b}e^{A_i(\gamma-\gamma_0)/kT} \tag{8}$$

where γ_0 refers to pure compound surface tension, is thermodynamically inconsistent leading to a contradiction with eq 2. Ostensibly, eq 8 is an integrated form of the Gibbs adsorption equation (1), but from eq 8 rederivation of adsorption equation leads to

$$\Gamma_1 \mathrm{d}\mu_{1,s} + \Gamma_2 \mathrm{d}\mu_{2,s} = 0 \tag{9}$$

that is consistent with the definition

$$\mu_{i,s} = \left(\frac{\partial G_s}{\partial n_{i,s}}\right)_{T,p,n_{j,s}} \tag{10}$$

and is not directly obtainable from measurement of thermodynamic variables because surface tension is not constant in this expression. Furthermore, partial molecular areas A_i are not directly measurable quantities while surface tension of mixture and the total surface area appearing in eq 1 via definition of Γ_i are. For further discussion, see refs 11, 23, and 32.

To make comparison of different models possible, partial molecular areas were taken as those used by Guggenheim,[11] namely $A_1 = 0.07$ nm^2 for water and $A_2 = 0.20$ nm^2 for all alcohol molecules. Because all alcohol molecules tend to extend their alkyl tails toward the vapor phase in water−alcohol surfaces,[17,33,34] the usage of same partial molecular areas for each of them can be judged to be correct. One must notice that we do not need to assume that all alcohol molecules form the same tilt angle θ (0°) with the normal of the surface: the same expectation value of A_i with respect to the distribution of θ will do when it comes to phenomenological models. And because we are not considering experimental determination of partial molecular areas, peculiarities noted in phenol molecule tilt angle[35] at similar setup do not play a role in determination of surface composition. Different values used in the literature for partial molecular areas of water and short-chain alcohols are collected in Table 1. For longer chain *n*-alcohols Fainerman et al.[36] report values for partial molecular areas not very different from that of *n*-propanol.

The partial molecular areas depend on the exact location of dividing surface. From the adsorption eq 1 one can deduce that

$$\Gamma_2 = -kT\frac{\mathrm{d}\gamma}{\mathrm{d}\ln a_2} \tag{11}$$

when the dividing surface is chosen via condition $\Gamma_1 = 0$, describing alcohol monolayer at the surface. Note, however, that from eq 3 we would have

$$A_2 = {\Gamma_2}^{-1} \tag{12}$$

which clearly does not make sense (but gives an upper limit for possible value of A_2). The problem here is that the Gibbs excess quantities are related with molecular numbers within a finite surface layer. Also, an assumption of alcohol monolayer at the surface makes the calculation of surface composition trivial by implementing $x_s = 1$. This assumption also makes it impossible to relate our observations of surface composition of the water−ethanol mixture to those obtained recently from computer simulations.[37−39]

4. Density Functional Theory of Binary Mixtures

The density functional method of classical fluids relies on a definition of Helmholtz free energy F (or grand potential Ω) as a function of the average number density distributions $\rho_i(\mathbf{r})$. We employ this formalism to a model binary mixture consisting of a monatomic and a diatomic component where each atom is described by a hard sphere with an attractive potential tail. The grand potential functional for this mixture is written as[40]

$$\begin{aligned}\beta\Omega[\rho_0(\mathbf{r}), \rho_1(\mathbf{r}), \rho_2(\mathbf{r})] = {} & \int \mathrm{d}\mathbf{r}\, \rho_0(\mathbf{r}) \ln \rho_0(\mathbf{r}) + \\ & \sum_{j=1}^{2}\int \mathrm{d}\mathbf{r}\, \rho_j(\mathbf{r}) \ln f_j(\mathbf{r}) + \int \mathrm{d}\mathbf{r}\, \Psi[\eta(\mathbf{r})]\rho_s(\mathbf{r}) - \\ & \int\int \mathrm{d}\mathbf{r}\, \mathrm{d}\mathbf{r}'\, s^{(2)}(|\mathbf{r}-\mathbf{r}'|)\, f_1(\mathbf{r})\, f_2(\mathbf{r}') + \frac{\beta}{2}\sum_{j,k=0}^{2} \\ & \int\int \mathrm{d}\mathbf{r}\, \mathrm{d}\mathbf{r}'\, \phi_{jk}(|\mathbf{r}-\mathbf{r}'|)\, \rho_j(\mathbf{r})\, \rho_k(\mathbf{r}') - \beta\sum_{j=0}^{2}\mu_j\int \rho_j(\mathbf{r})\, \mathrm{d}\mathbf{r}\end{aligned} \tag{13}$$

where $\beta = 1/k_BT$, Ψ is the excess free energy per particle over the ideal gas, $\rho_s(\mathbf{r})$ is the total density, and $\eta(\mathbf{r}) = (\pi\sigma^3/6)\rho_s(\mathbf{r})$ is the packing fraction of hard spheres. In the following we assume that the hard spheres have equal diameters, i.e., $\sigma_{ij} = \sigma$ $\forall$ i, j. Functions $f_i(\mathbf{r})$ correspond to activities of the atomic sites, and the interaction potential between atoms i and j is given by ϕ_{ij}. It should be noted that the densities in this formalism are the densities of the interaction sites, i.e., the atomic parts of the molecules with ρ_0 corresponding to monatomic component and ρ_1 and ρ_2 to the two sites of the diatomic molecule.

The attractive interaction is given by the Lennard-Jones (LJ) potential

$$\phi_{ij}^{\mathrm{LJ}}(r) = 4\epsilon_{ij}\left[\left(\frac{\sigma_{ij}}{r}\right)^{12} - \left(\frac{\sigma_{ij}}{r}\right)^{6}\right] \quad (i, j = 0, 1, 2) \tag{14}$$

where σ_{ij} are the length parameters and ϵ_{ij} the energy parameters. The excess free energy of the hard-sphere fluid is obtained from the Carnahan−Starling expression.[41] Rigid bonds are assumed between the sites in the diatomic molecules with the correlation function given by $s^{(2)}(r) = (4\pi\sigma^2)^{-1}\delta(r - \sigma)$.

The density profiles for a gas−liquid interface are obtained by minimizing eq 13 with respect to functions $\rho_i(\mathbf{r})$ and $f_i(\mathbf{r})$ and solving the resulting equations numerically in planar geometry. The surface tension is then calculated from

$$\gamma A = \Omega[\{\rho_i(\mathbf{r})\}] - \Omega_e \tag{15}$$

where A is the area of the interface and Ω_e is the grand potential evaluated at the coexisting bulk densities.

The equilibrium values for densities are obtained from equation-of-state relations for pressure P and chemical potentials μ_i at the limit of homogeneous bulk. Because $P = -\Omega/V$, eq 13 reduces to

$$P = k_BT(\rho_0 + \rho) + k_BT\Psi'\upsilon{\rho_s}^2 - \frac{1}{2}\sum_{i,j=0}^{2}\alpha_{ij}\rho_i\rho_j \tag{16}$$

where $\alpha_{ij} = -\int \mathrm{d}\mathbf{r}\, \phi_{ij}^{\mathrm{LJ}}(r)$ and $\rho_1 = \rho_2 = \rho$. On the other hand, the equations resulting from the above-mentioned minimization give the chemical potentials at the homogeneous limit as

$$\mu_0 = k_BT\ln\rho_0 + U_0 \tag{17}$$

$$\mu = \mu_1 + \mu_2 = k_BT\ln\rho + U_1 + U_2 \tag{18}$$

with

$$\beta U_i = \Psi + \Psi'\upsilon\rho_s - \beta\sum_{j=0}^{2}\alpha_{ij}\rho_j \tag{19}$$

In our model fluids the LJ energy parameters are given by

$$\epsilon_{ij} = (1 - k_{ij})\sqrt{\epsilon_{ii}\epsilon_{jj}} \tag{20}$$

where the parameter k_{ij} quantifies the deviation of the cross interaction energy parameters from the usual geometric mean rule. The desired phase and interfacial behavior can be sought by varying k_{ij}. The typical features of water−alcohol mixtures are captured by weakening the total interaction between the monatomic molecule (a "monomer") and the diatomic molecule (a "dimer") so that one end of the "dimer" is more attracted to "monomer" than the other. The former condition causes the "dimer" to enrich on the gas−liquid surface while the latter gives rise to the orientation of "dimers" perpendicular to surface. In terms of parameters k_{ij} these requirements are expressed as $k_{01} + k_{02} > 0$ and $k_{01}k_{02} < 0$. Extensive work on phase behavior and nucleation of these kind of fluid mixtures has been done earlier by DFT[8,40,42,43] and Monte Carlo simulations.[44]

TABLE 2: Parameters k_{ij} and the Upper Critical Solution Temperature T_{cr}^{U} for the Two Fluid Systems

fluid	k_{01}	k_{02}	k_{12}	T_{cr}^{U}/ϵ
I	−0.3	0.374	0	0.693
II	−0.337	0.337	0	0.449

5. Results

5.1. Determination of Surface Phase from DFT. In this section we investigate how the location and the composition of the surface phase can be determined from the DFT density profiles for two model fluids. The parameters k_{ij} and the upper critical solution temperature T_{cr}^{U} of the fluids are specified in Table 2. The energy parameters are $\epsilon_{11} = \epsilon_{22} = 0.6\epsilon$ for both fluids, where $\epsilon \equiv \epsilon_{00}$, and the hard-sphere diameter σ is the same for all components. The fluids are studied at temperature $T/\epsilon = 0.7$, where fluid I is very close to liquid−liquid segregation and barely mixes at medium compositions, whereas

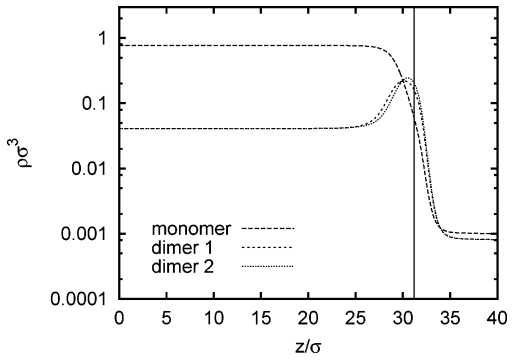

Figure 1. Liquid-vapor density profiles for the fluid mixture I when the bulk mole fraction of dimers is $x_b = 0.05$. Profiles for the monomer component and for the both ends of the dimer are shown. The vertical line shows the location of the equimolar surface z_e.

fluid II behaves in a more "ideal" manner. Fluid I was studied for gas-phase nucleation in ref 8. In the following we use subscript M for the monomer molecule while D indicates dimer with D1 and D2 the two ends of the dimer.

Typical liquid−vapor density profiles for fluid I are shown in Figure 1. The dimer molecules enrich on the surface with the densities of the D1 and D2 atoms peaking approximately σ apart. This indicates orientation of the dimers with the symmetry axis perpendicular to the surface. In principle, the densities and composition can be determined directly from the density profiles. To do that, however, we must first define the surfaces which divide vapor from liquid and the surface phase from the bulk liquid.

A conceivable choice for the division between vapor and liquid is the equimolar surface z_e given by the condition

$$\upsilon_M \Gamma_M + \upsilon_D \Gamma_D = 0 \tag{21}$$

where the partial molecular volumes are calculated from

$$\upsilon_i = \left(\frac{\partial \mu_i}{\partial P}\right)_{x,T} \tag{22}$$

and the excess number of molecules from

$$\Gamma_i = \int_0^\infty \mathrm{d}z\, (\rho_i(z) - \rho_{i,v}) - \Delta\rho_i z_e \quad (i = \mathrm{M, D}) \tag{23}$$

where $\Delta\rho_i = \rho_{i,l} - \rho_{i,v}$ with $\rho_{i,l}$ and $\rho_{i,v}$ the densities of component i in the homogeneous liquid and vapor, respectively. The z-axis is normal to the surface, and the origin is sufficiently far away from interface in the bulk liquid. In Figure 1 the equimolar surface is shown as a vertical line.

The surface composition x_s can be considered as a local quantity which is related to a particular surface property or a quantity which is averaged over a distance. In the local scheme there are three obvious choices to determine x_s. It could be taken to be the same as the composition at z_e or associated with the maximum of the local composition $x(z) = \rho_D(z)/(\rho_M(z) + \rho_D(z))$. Figure 2 shows $x(z)$ as a function of distance with the equimolar surface at the same position. It can be seen that the maximum of the curves is located on the vapor side of the surface z_e; interestingly, the distance between z_e and the maximum of the curves in Figure 2 does not depend on the bulk mole fraction. The third choice is to determine the maximum of the average value of the local dimer site densities, which would relate x_s to the abundance of dimers at liquidlike densities. Nevertheless, the knowledge of the spatial extent of the molecules is lost in all local schemes.

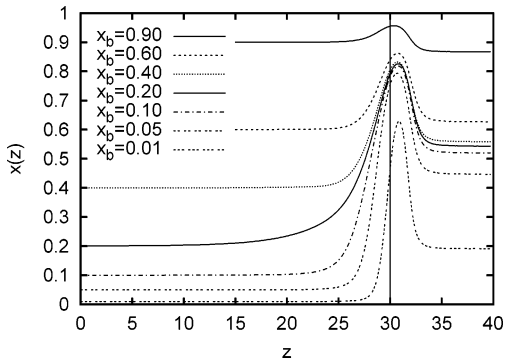

Figure 2. Local mole fraction of dimers as a function of distance. Equimolar surface is fixed at 30σ.

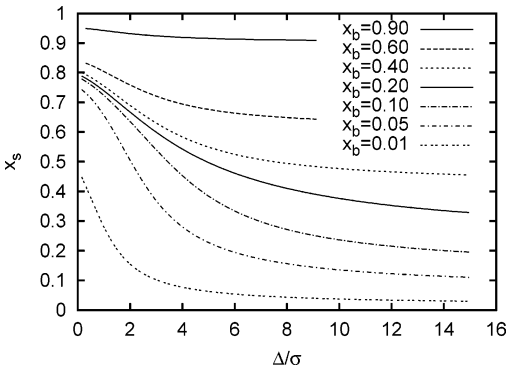

Figure 3. Dependence of the surface mole fraction of dimers on the thickness of the surface layer for several bulk mole fractions. The integration of the density profiles is performed from $z_e - \Delta$ to z_e.

When compared to experimental approaches, a more realistic picture of the surface phase involves a finite slice of the surface which is located at least partly at liquidlike densities. If the equimolar surface z_e is assumed as the dividing surface between vapor and liquid, the surface phase can be taken to extend a distance Δ from z_e to the bulk liquid or, more or less symmetrically, to both sides of z_e. The density profiles are then integrated over the distance Δ to yield the number of particles in the surface phase per unit area, Γ_i, from which x_s can be determined. In the spirit of Guggenheim[15] we assume that the surface phase consists of a single molecular layer. However, this leaves the exact position of the surface layer with respect to z_e undetermined. Moreover, the molecules in our model fluids are not the same size, which requires a method to calculate Δ.

The surface composition as a function of Δ is shown in Figure 3 for several bulk mole fractions x_b. The density profiles were integrated from $z_e - \Delta$ to z_e. The maximum of x_s is reached when Δ tends to zero. A quite strong dependence on x_s is found when the bulk mole fraction is small, because then the dimers are mainly located close to the surface. The dimer site density profiles become more spread out with increasing x_b which contributes to a weaker dependence on Δ at large x_b.

A dividing surface between the liquid surface and the bulk liquid can be found where the adsorption of the solvent component (monomer) vanishes

$$\Gamma_M = 0 \tag{24}$$

We could then locate the surface phase between dividing surfaces given by eqs 21 and 24. However, the surface layer thus defined can be quite thick at high solute (dimer) mole fractions, and since we are mainly interested in unimolecular interfacial layers when the DFT calculations are compared to

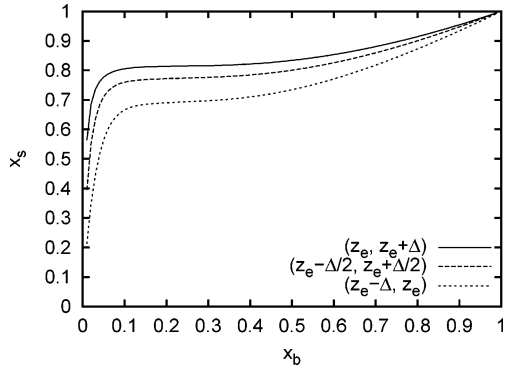

Figure 4. Surface mole fraction of dimers, x_s, as a function of the bulk mole fraction. Three possible choices for the location of the surface layer are considered. The boundaries of the surface layer are shown in the legend. The thickness of the layer is the diameter of one average molecule (see text for details).

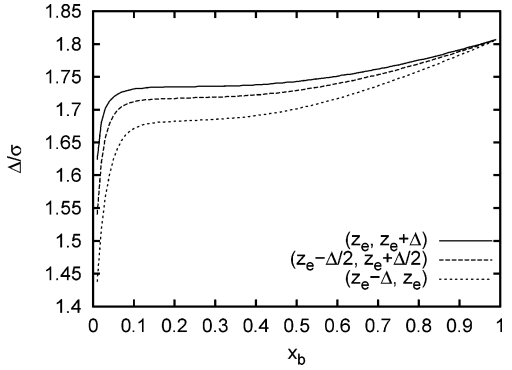

Figure 5. Thickness of the surface layer as a function of the bulk mole fraction. The curves correspond to those of Figure 4.

semiempirical models, the definition given by eq 24 is not very useful to us (see also the argumentation in section 3).

In our model fluids, as well as in real surfactant mixtures, the solute molecules are oriented normal to the surface. Assuming that the thickness of the surface layer is one molecular diameter, the simplest choice is then to set $\Delta = 2\sigma$, i.e., the length of the dimer molecule. However, the surface phase also contains solvent molecules with the hard-sphere diameter σ. To find a compromise between the different molecular sizes, we have applied an iterative procedure to determine diameter of an "average" molecule in the surface phase. The volume of the average molecule, v_{av}, is a weighted sum of volumes of the partial molecular volumes of pure substances

$$v_{av} = (1 - x_s)v_M + x_s v_D \tag{25}$$

The thickness of the surface, the diameter of the average molecule, and the surface mole fraction of dimers are solved simultaneously with the bulk liquid composition as an initial value. Equation 25 gives the diameter of the molecule, which is equal to Δ. Integration of the density profiles over Δ yields a new value for x_s, which is then substituted to eq 25. This process is continued until both the integration and eq 25 give the same x_s.

The surface mole fraction of dimers determined using this method is illustrated in Figure 4. The dotted line shows the composition assuming that the surface phase extends from z_e toward bulk liquid, as was the case in Figure 3. The dashed line shows x_s when the integration is performed symmetrically around z_e. For comparison, asymmetric integration from z_e toward the vapor is shown as a solid line.

The thickness of the surface, which is shown in Figure 5 for the three cases of Figure 4, increases very rapidly with the bulk mole fraction x_b, which results from the surface enrichment even at low x_b. For $x_b > 0.1$ there is less increase in surface thickness because the surface becomes saturated with dimers.

Both the surface mole fraction and the thickness of the surface increase when more of the vapor phase is taken within the integration limits. This is not surprising since the local composition peaks on the vapor side of z_e, as shown in Figure 2. On the other hand, the low densities on the vapor side contribute less to the integration, and the net effect is not as drastic as could be expected. Since the surface layer is more related to the liquid than to the vapor phase, we have taken the asymmetrically integrated layer from z_e toward the liquid as a reference case, which is used for comparison with the phenomenological models in the following.

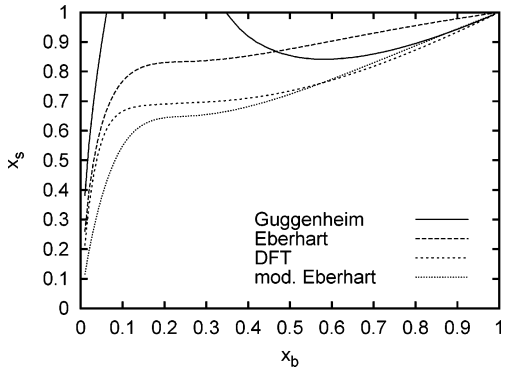

Figure 6. Variation of the surface mole fraction of dimer x_s with the mole fraction of dimers in the bulk liquid for mixture I. DFT calculations and phenomenological models (Guggenheim, eqs 1−3; Eberhart, eq 4; modified Eberhart, eq 5) are compared. The surface layer is assumed to extend the diameter of an average molecule from the equimolar surface to liquid.

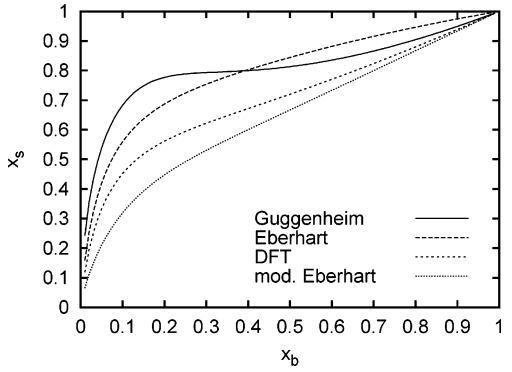

Figure 7. Same as Figure 6 for mixture II.

5.2. Phenomenological Models. The surface composition is determined as a function of bulk composition and temperature from eqs 1−5. Comparisons of different methods for model fluids with DFT results are presented in Figures 6 and 7 and for water−alcohol mixtures in Figures 8−12. In the case of the Guggenheim model, we have also demonstrated the effects of different activity coefficient parametrizations for water−ethanol and water−*n*-propanol mixtures (Figures 10 and 12) and the effect of temperature for water−ethanol mixture (Figure 11). For activity coefficients, van Laar equations from ref 28 for methanol and from ref 23 for ethanol and *n*-propanol are used unless otherwise indicated. The DFT calculation of the surface compositions was done using the method of average molecule, as described in the preceding section. Because the equation of state is available everywhere in DFT calculations, the Guggenheim curve was computed directly from eqs 1 and 3. Equal

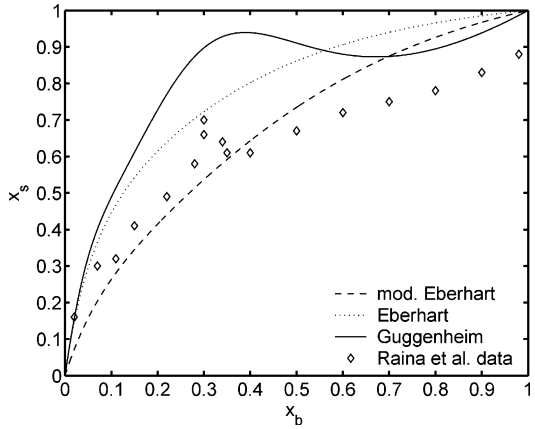

Figure 8. Surface mole fraction of methanol x_s in the water−methanol mixture as a function of the bulk mole fraction of methanol at 298 K. Different phenomenological models are compared at 298 K. Experimental results from Raina et al.[14] are also included.

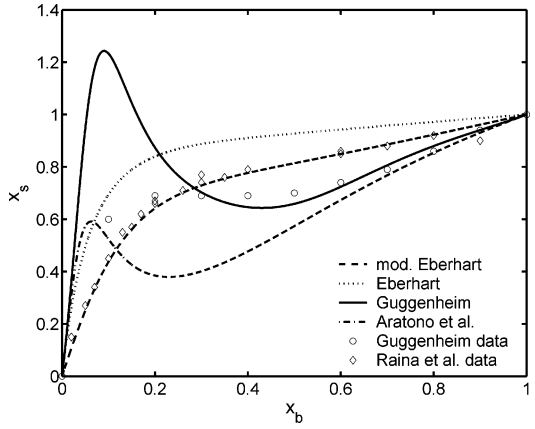

Figure 9. Same as Figure 8 for the water−ethanol mixture. Also data by the method described by Aratono et al.[18] with the same set of parametrizations as the other models and that calculated by Guggenheim[11] and measured by Raina et al.[14] are included.

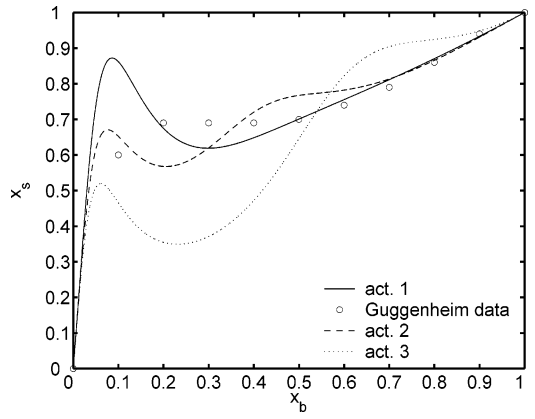

Figure 10. Effect of different activity parametrizations on the (x_b, x_s) plot in the case of the water−ethanol mixture at 298 K. Act. 1 refers to activity parametrization of Strey et al.,[23] act. 2 to that of d'Avila and Silva,[30] and act. 3 to that of Gaulhofer et al.[31]

partial surface areas were assumed for monomers and dimers, corresponding to dimer molecules oriented perpendicular to the surface.

The surface composition estimates from the Guggenheim model are in striking discrepancy with the DFT results in Figure 6. The Guggenheim curve even exceeds $x_s = 1$ when $0.07 < x_b < 0.35$, which, of course, contradicts the definition of mole fraction. The model is relatively insensitive to changes in A_M,

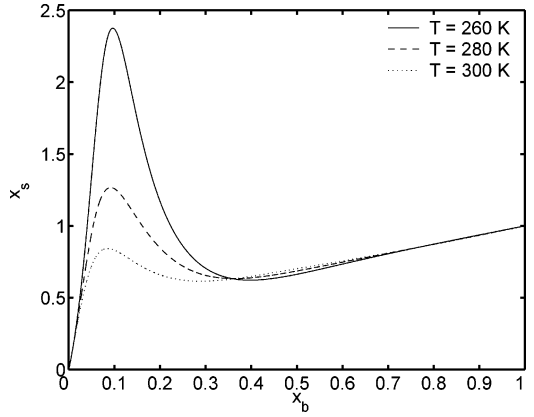

Figure 11. Effect of temperature to the surface mole fraction of ethanol x_s with the bulk mole fraction of ethanol in the water−ethanol mixture at different temperatures using the Guggenheim model.

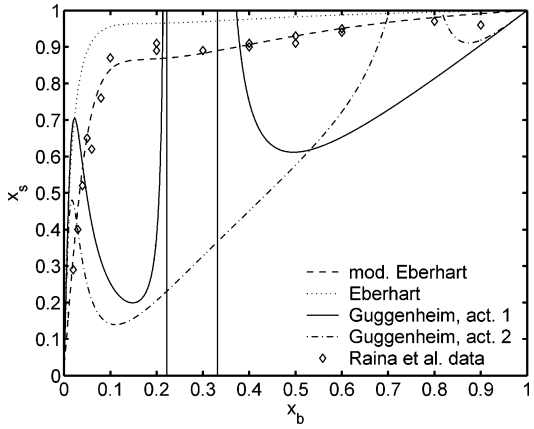

Figure 12. Same as Figure 8 for the water−*n*-propanol mixture. Act. 1 refers to parametrization from Strey et al.[23] and act. 2 to that of Flageollet et al.[28] Experimental results from Raina et al.[14] are also included.

as Guggenheim already observed for water in the water−ethanol system.[15] Changes in A_D due to different orientations of molecules do not affect the results qualitatively. The value of A_D has to be decreased to unreasonably small magnitude to keep the surface composition in the range $0 \le x_s \le 1$. Water−alcohol mixtures show similar behavior in Figures 8, 9, and 12.

When classifying different situations according to the surfactant solubility in solvent, we see that the increased solubility due to shortening of alkyl chain or increasing temperature generally amplifies mixing between the bulk and the surface in water−alcohol mixtures. This attenuates stratification in the vicinity of the interface. Then the assumptions behind the Guggenheim model, i.e., coincidence of dividing surfaces in eqs 1 and 3, become more realistic, and different models for surface composition do converge. In the case of model fluids I and II, we observe the same phenomenon with the system II giving more realistic values for x_s; however, also in this case the predictions of the Guggenheim model are rather poor. In water−alcohol systems these effects are enhanced by the effects of different activity parametrizations. Nevertheless, the differences in predicted activities are always less than 10% and generally much less at 298 K. For the most surface active mixture, water−*n*-propanol (Figure 12), the Guggenheim model yields surface mole fractions that are either greater than unity or negative.

On the basis of Figures 6−9 and Figure 12, Eberhart and modified Eberhart models (eqs 4 and 5, respectively) both give physically acceptable results for both model fluids and water−

alcohol mixtures. We also tried a variant of the modified Eberhart model where the surface mole fraction is weighted with partial molecular areas determined from partial molecular volumes of eq 22. Of these three methods, eq 5 is in best agreement with DFT calculations, although the model weighted with partial molecular areas seems to reproduce the lowest surface compositions better. The modified Eberhart model can be further amended by evaluating the partial molecular volumes at the composition of the surface layer; however, the resulting change in x_s is 5% at most. Eberhart's original model overestimates the DFT values at all bulk compositions.

It is notable that the modified Eberhart model, which gives best estimates in comparison with DFT calculations, has been experimentally proven for water−alcohol mixtures.[13,14] However, the experimental setup used in refs 13 and 14 provides knowledge about the nonequilibrium, evaporating surface instead of true equilibrium surface, for which different phenomenological models that use equilibrium values of thermodynamic variables are adequate. Still, the results from DFT calculations seem to justify the experimental results, especially when anomalies in (x_b, x_s) curve of the water−methanol mixture can be explained from the change in structure of hydrogen-bonding network.[13,45,46]

In a rather recent effort to model surface concentrations, Aratono et al.[18] introduced a H-surface from conditions

$$\Gamma_a^H = 0 \quad \text{and} \quad \Gamma_1^H + \Gamma_2^H = 0$$

where subscript "a" stands for air. Then they calculated the corresponding surface concentrations for the surface defined by eq 3 for the water−ethanol system via thermodynamic transformations between these two surfaces. The predictions of this model are shown for the water−ethanol system in Figure 9. Comparing the curves in Figure 9, we find that there is a qualitative similarity with results of Aratono et al. and the ones from the Guggenheim model. The similarity is not, however, a quantitative one because of the slightly different partial molecular areas used and because the activity model[31] used by Aratono et al.[18] is thermodynamically inconsistent, as noted in section 3. Still, the method by Aratono et al. gives realistic values for x_s when consistent data sets are used and, in this respect, is superior to the Guggenheim model. The method is also less sensitive to different activity parametrizations due to the logarithmic differentiation procedure. However, it is not in harmony with experimental values[14] or our results from DFT calculations.

5.3. Comparison with Numerical Simulations. There exists simulation work on surfactant systems, in particular on mixtures of water and ethanol, which can be compared with our results. Tarek et al.[37] performed molecular dynamics simulations and presented density profiles at one liquid composition. They observed an ethanol depletion layer beneath the layer of surface excess. Our DFT results (Figure 2) do not show such a feature as the dimer mole fraction is seen to decrease monotonically to the bulk value on the liquid side of the mole fraction maximum. It is conceivable that the more complex nature of interaction potentials in the simulations may induce effects which are not observed in our simple DFT model. However, a more comprehensive study done recently by Stewart et al.[47] indicates that the depletion layer is very weak or even nonexistent.

To further compare our results with simulations, we have used the four density profiles and the fitting functions provided by Stewart et al.[47] to calculate both the local mole fraction and the integrated surface composition of the water−ethanol system. Figure 13 shows the local composition as a function of distance.

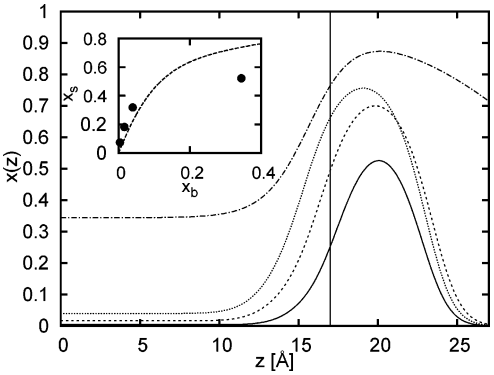

Figure 13. Local mole fraction at the vapor−liquid boundary of the water−ethanol mixture obtained from the density profiles of Stewart et al.[47] The inset shows the surface mole fraction as a function of bulk mole fraction (dots). Predictions of the modified Eberhart model for the real water−ethanol mixture are also shown (dashed line).

The equimolar surface z_e (shown as a vertical line) is also calculated from the profiles, and the profiles have been adjusted so that the equimolar surface coincides for all four cases. It is interesting to notice that the distance between the equimolar surface and the maximum of local composition is almost constant and a bit less than half the length of an ethanol molecule (6 Å). Similar observations were made of our model fluid in Figure 2. It seems that the constancy of this distance as a function of bulk mole fraction is characteristic of surfactant systems and dependent on the length of the chain molecule.

The inset in Figure 13 shows the surface mole fraction of ethanol which has been obtained by integrating the profiles from $z_e - \Delta$ to z_e, where Δ is the diameter of an average molecule. Also shown are the predictions of the modified form of the Eberhart formula. At low mole fractions the simulated and the model results are in good agreement. The rightmost point, however, is substantially lower than the model value. This must not be considered a flaw of the model: the model results are for a real water−ethanol mixture, whereas the simulated surface excesses are lower than experimental values owing to differences between simulated and experimental thermodynamic properties of the solution.[47] Note that curiously low local mole fractions at the vapor side result from the omission of vapor phase from the fitting functions. This does not affect the integrated surface mole fractions because the densities to the right from the mole fraction maxima are very low.

6. Discussion and Conclusions

We have compared several phenomenological models to calculate surface compositions for planar vapor−liquid interfaces of binary surfactant mixtures. The models are tested using model hard-sphere fluids and real water−alcohol mixtures. The results for the model fluids are obtained from density functional theory. Different possibilities for determining the extent of surface phase are discussed in connection with density profiles from DFT. The surface layer extending the diameter of one average molecule from the equimolar surface defined by eq 21 toward the bulk liquid is taken as a reference case. For water−alcohol mixtures, the surface layer is specified via partial molecular areas at the reference surface.

The model proposed by Laaksonen and Kulmala (modified Eberhart model) seems to be in quite good agreement with the DFT calculations and yields somewhat better predictions than the original model by Eberhart. The superiority of the modified Eberhart model is further confirmed by experimental and simulation results. The measurements of Raina et al.[13,14] follow

closely the predictions of the model. The integrated surface surface composition based on the molecular dynamics simulations of Stewart et al.[47] is also in accordance with the model results. These facts together not only support the modified Eberhart model but also give quite strong indication that our definition of surface layer corresponds to that sampled by the experimental method.

The Guggenheim model is the poorest of the models considered in this study; it is completely unusable for mixtures with high surface activity, as attested by both the DFT calculations and application to water−alcohol mixtures.

The failure of the Guggenheim model results from a mismatch between the concepts of Γ_i in different contexts. The Guggenheim model assumes that Γ_i in eqs 1 and 3 are physical quantities: the number of molecules in a finite surface layer which, in principle, can be measured or observed. However, the Gibbs adsorption equation does not give Γ_i this specific interpretation; they are just terms which measure the excess number of molecules with respect to some dividing surface. For example, the equation for equimolar surface, eq 21, defines a surface where Γ_1 and Γ_2 always have opposite signs. Equation 3 refers to another surface, but there is no reason to presume that both Γ_i are positive. In fact, Γ_M is negative for the model fluid I in that part of the surface composition plot where $x_s > 1$.

For water−alcohol mixtures, the anomalies of x_s given by the Guggenheim model seem to appear approximately at the same bulk mole fractions where there is a deep minimum in partial molar volume vs x_b plot. However, in the case of *n*-propanol, the effect depends so heavily on the activity model used that no conclusions can be drawn, and the existence of two anomalies in thermodynamic properties at the same range of mole fractions has to be considered as a coincidence. Furthermore, the strong dependence on activity parametrization used makes the Guggenheim model even more unsatisfactory: a probable reason for the difference between Guggenheim's[11] and our calculations (Figure 9). For surface tension and partial molecular (or molar) volumes, the parametrizations used are mathematically more convenient so that the Eberhart and modified Eberhart models do not suffer from similar problems.

Acknowledgment. This work was supported by the Academy of Finland. J.M. thanks Dr. M. Noppel for comments on the manuscript.

References and Notes

(1) Schürch, S.; Green, F. H. Y.; Bachofen, H. *Biochim. Biophys. Acta* **1998**, *1408*, 180.
(2) Brimblecombe, P.; Latif, M. T. *Environ. Chem.* **2004**, *1*, 11.
(3) Sorjamaa, R.; Svenningsson, B.; Raatikainen, T.; Henning, S.; Bilde, M.; Laaksonen, A. *Atmos. Chem. Phys.* **2004**, *4*, 2107.
(4) Tuck, A. *Surv. Geophys.* **2002**, *23*, 379.
(5) Strey, R.; Viisanen, Y.; Wagner, P. E. *J. Chem. Phys.* **1995**, *103*, 4333.
(6) Kulmala, M.; Lauri, A.; Vehkamäki, H.; Laaksonen, A.; Petersen, D.; Wagner, P. E. *J. Phys. Chem. B* **2001**, *195*, 11800.
(7) Laaksonen, A.; Kulmala, M. *J. Chem. Phys.* **1991**, *95*, 6745.
(8) Laaksonen, A.; Napari, I. *J. Phys. Chem. B* **2001**, *105*, 11678.
(9) Laaksonen, A.; McGraw, R.; Vehkamäki, H. *J. Chem. Phys.* **1999**, *111*, 2019.
(10) Laaksonen, A. *J. Chem. Phys.* **1992**, *97*, 1983.
(11) Guggenheim, E. A. *Thermodynamics*, 3rd ed.; North-Holland: Amsterdam, 1967.
(12) Eberhart, J. G. *J. Phys. Chem.* **1966**, *70*, 1183.
(13) Raina, G.; Kulkarni, G. U.; Rao, C. N. R. *Int. J. Mass Spectrom.* **2001**, *212*, 267.
(14) Raina, G.; Kulkarni, G. U.; Rao, C. N. R. *J. Phys. Chem. A* **2001**, *105*, 10204.
(15) Guggenheim, E. A.; Adam, N. K. *Proc. R. Soc. London A* **1933**, *139*, 218.
(16) Eriksson, J. C. *Ark. Kemi* **1966**, *26*, 49.
(17) Tronel-Peyroz, E.; Douillard, J. M.; Tenebre, L.; Bennes, R.; Privat, M. *Langmuir* **1987**, *3*, 1027.
(18) Aratono, M.; Toyomasu, T.; Villeneuve, M.; Uchizono, Y.; Takiue, T.; Motomura, K.; Ikeda, N. *J. Colloid Interface Sci.* **1997**, *191*, 146.
(19) Defay, R.; Prigogine, I. *Surface Tension and Adsorption*; Longmans: London, 1966.
(20) Teitelbaum, B. V.; Gortalova, T. A.; Siderova, E. E. *Zh. Fiz. Khim.* [*Russ. J. Phys. Chem.*] **1951**, *25*, 911.
(21) Timmermans, J. *The Physico-Chemical Constants of Binary Systems in Concentrated Solutions*; Interscience Publishers: New York, 1960.
(22) Vázquez, G.; Alvarez, E.; Navaza, J. M. *J. Chem. Eng. Data* **1995**, *40*, 611.
(23) Strey, R.; Viisanen, Y.; Aratono, M.; Kratohvil, J. P.; Yin, Q.; Friberg, S. E. *J. Phys. Chem. B* **1999**, *103*, 9112.
(24) Vesala, T. Philos. Lic. Thesis, University of Helsinki, Helsinki, Finland, 1990.
(25) Preining, O.; Wagner, P. E.; Pohl, F. G.; Szymanski, W. *Heterogeneous Nucleation and Droplet Growth*; University of Vienna, Institute of Experimental Physics: Vienna, Austria, 1981.
(26) Perry, R. H., Chilton, C. H., Eds. *Chemical Engineer's Handbook*, 5th ed.; McGraw-Hill: Auckland, 1973; pp 3−83.
(27) Dethlefsen, C.; Sørensen, P. G.; Hvidt, A. *J. Solution Chem.* **1984**, *13*, 191.
(28) Flageollet, C.; Dinh Cao, M.; Mirabel, P. *J. Chem. Phys.* **1980**, *72*, 544.
(29) Note that in eq 4 in ref 28 *A* and *B* must be changed when $i = 2$.
(30) d'Avila, S. G.; Silva, R. S. F. *J. Chem. Eng. Data* **1970**, *15*, 421.
(31) Gaulhofer, A.; Kolbe, B.; Gmehling, J. *Fluid Phase Equilib.* **1988**, *39*, 193.
(32) Sugimoto, T. *J. Colloid Interface Sci.* **1996**, *181*, 259.
(33) Li, Z. X.; Lu, J. R.; Styrkas, D. A.; Thomas, R. K.; Rennie, A. R.; Penfold, J. *Mol. Phys.* **1993**, *80*, 925.
(34) Stanners, C. D.; Du, Q.; Chin, R. P.; Cremer, P.; Somorjai, G. A.; Shen, Y.-R. *Chem. Phys. Lett.* **1995**, *232*, 407.
(35) Li, Z. X.; Thomas, R. K.; Rennie, A. R.; Penfold, J. *J. Phys. Chem. B* **1998**, *102*, 185.
(36) Fainerman, V. B.; Miller, R.; Möhwald, H. *J. Phys. Chem. B* **2002**, *106*, 809.
(37) Tarek, M.; Tobias, D. J.; Klein, M. L. *J. Chem Soc., Faraday Trans.* **1996**, *92*, 559.
(38) Tarek, M.; Tobias, D. J.; Klein, M. L. *Physica A* **1996**, *231*, 117.
(39) Tarek, M. Personal communication.
(40) Napari, I.; Laaksonen, A.; Strey, R. *J. Chem. Phys.* **2000**, *113*, 4476.
(41) Mansoori, G. A.; Carnahan, N. F.; Starling, K. E.; Leland, T. W. *J. Chem. Phys.* **1971**, *54*, 1523.
(42) Napari, I.; Laaksonen, A. *Phys. Rev. Lett.* **2000**, *84*, 2184.
(43) Napari, I.; Laaksonen, A.; Strey, R. *J. Chem. Phys.* **2000**, *113*, 4480.
(44) Yoo, S.; Oh, J.; Zeng, X. C. *J. Chem. Phys.* **2001**, *115*, 8518.
(45) Takamuku, T.; Yamaguchi, T.; Asato, M.; Matsumoto, M.; Nishi, N. *Z. Naturforsch.* **2000**, *55a*, 513.
(46) Dixit, S.; Poon, W. C. K.; Crain, J. *J. Phys.: Condens. Matter* **2000**, *12*, L323.
(47) Stewart, E.; Shields, R. L.; Taylor, R. S. *J. Phys. Chem. B* **2003**, *107*, 2333.